

# Last glacial wind regime in southwest France derived from dunes, grain-size gradients and loess geochemistry.

Luca Sitzia, Pascal Bertran, Adriana Sima, Philippe Chery, Alain Queffelec, Denis-Didier Rousseau

## Supplementary data

### 1. Grain-size analysis

The pre-treatment of samples for particle-size analysis included i) suspension in sodium hexametaphosphate (5 g/L) and hydrogen peroxide (35%) during 12 hours, and ii) 60 seconds of ultrasonification in the microgranulometer to achieve optimal dispersion. We used a HORIBA LA950 (0.01 $\mu$ m - 3000 $\mu$ m) laser microgranulometer and analysed the data with the NextSpec 7.10 software. The Mie solution to Maxwell's equations (also called Lorenz-Mie or Lorenz-Mie-Debye solution, Hergert and Wriedt, 2012) provided the basis for calculating the particle size (Mie, 1908) as is recommended by the ISO committee (Jones, 2003; ISO, 2009). We applied this solution to calculate the particle-size distribution in aqueous solution (refractive index 1,333) and chose a refractive index for the particles of 1.55 - 0.01i. This value gave the best fit between the measured diffracted light pattern and the iteratively-calculated one as indicated by the R parameter (eq. 1) (Bullimer, 2013).

$$R = \frac{1}{N} \sum_{i=1}^N \left\{ \frac{1}{y(x_i)} |y_i - y(x_i)| \right\} \quad (1)$$

$N$  = The number of detectors used for the calculation

$y_i$  = The measured scattered light at each channel ( $i$ ) of the detector

$y(x_i)$  = The calculated scattered light at each channel ( $i$ ) of the detector based on the chosen refractive index kernel and the reported particle-size distribution.

The Fraunhofer approximation to Maxwell's equation, despite its general use in particle-size analysis, is far from allowing such a good fit (de Boer et al., 1987; Bullimer, 2013). To demonstrate the impact of the choice of the algorithm in particle-size analysis by laser diffraction, we calculated the size distribution for some representative samples by using different algorithms and refractive indices on the same measurement made by the microgranulometer. The ternary plot (fig. SI\_1) shows how different can be the compositions obtained. As shown by the sample "Pot-aux-Pins", which is mostly sand, the Fraunhofer approximation is correct for large particles and the particle-size distributions of sandy samples are similar whatever the algorithm used. In contrast, finer-grained samples give strongly scattered results. Figure SI\_3 and Table SI\_1 point to a poor fit (high R value) of the calculated signal with the measured one for the high angles of diffraction (i.e. for fine-grained particles) using the Fraunhofer algorithm. For the Mie algorithm, the particle size distribution (Fig. SI\_2) is also strongly influenced by the refractive index chosen. The number and size of the modes, and the proportion of the different size classes vary significantly according to the refractive index (Table SI\_1).

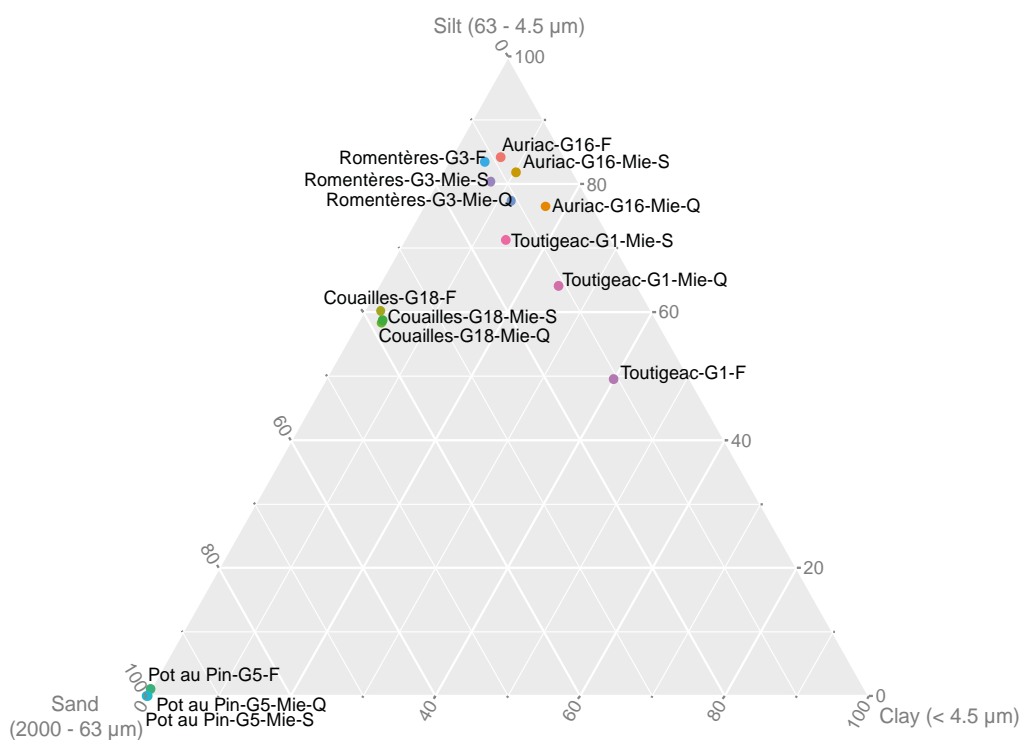


Figure SI\_1: Ternary diagram where the particle-size distributions calculated with the different algorithms and refractive indices are plotted. F: Fraunhofer, Mie-Q: Mie with the refractive index of quartz (1.45 - 0.00i), Mie-S: Mie with the refractive index of sediment (1.55 - 0.01i).

Sample-Algorithm	R	D10 (μm)	D50 (μm)	D90 (μm)	% Sand (2000-63 μm)	% Silt (63-4,5 μm)	% Clay (<4,5μ)
Auriac-G16-F	0,1292	5,2937	14,4613	59,0022	8,8659	84,2154	6,92
Auriac-G16-Mie-Q	0,072214	2,8817	20,5694	52,032	6,5025	76,5372	16,96
Auriac-G16-Mie-S	0,035178	4,4275	16,7085	55,7339	7,9268	81,863	10,21
Toutigeac-G1-F	0,17948	1,5858	8,3543	65,3287	10,5859	49,5153	39,9
Toutigeac-G1-Mie-Q	0,071635	1,0649	20,4792	66,832	10,9141	64,1188	24,97
Toutigeac-G1-Mie-S	0,059117	3,3708	16,968	87,2931	14,6276	71,264	14,11

Table SI\_1: R parameter and sedimentological values for calculations using the different algorithms for two samples (Auriac-G16 and Toutigeac-G1).

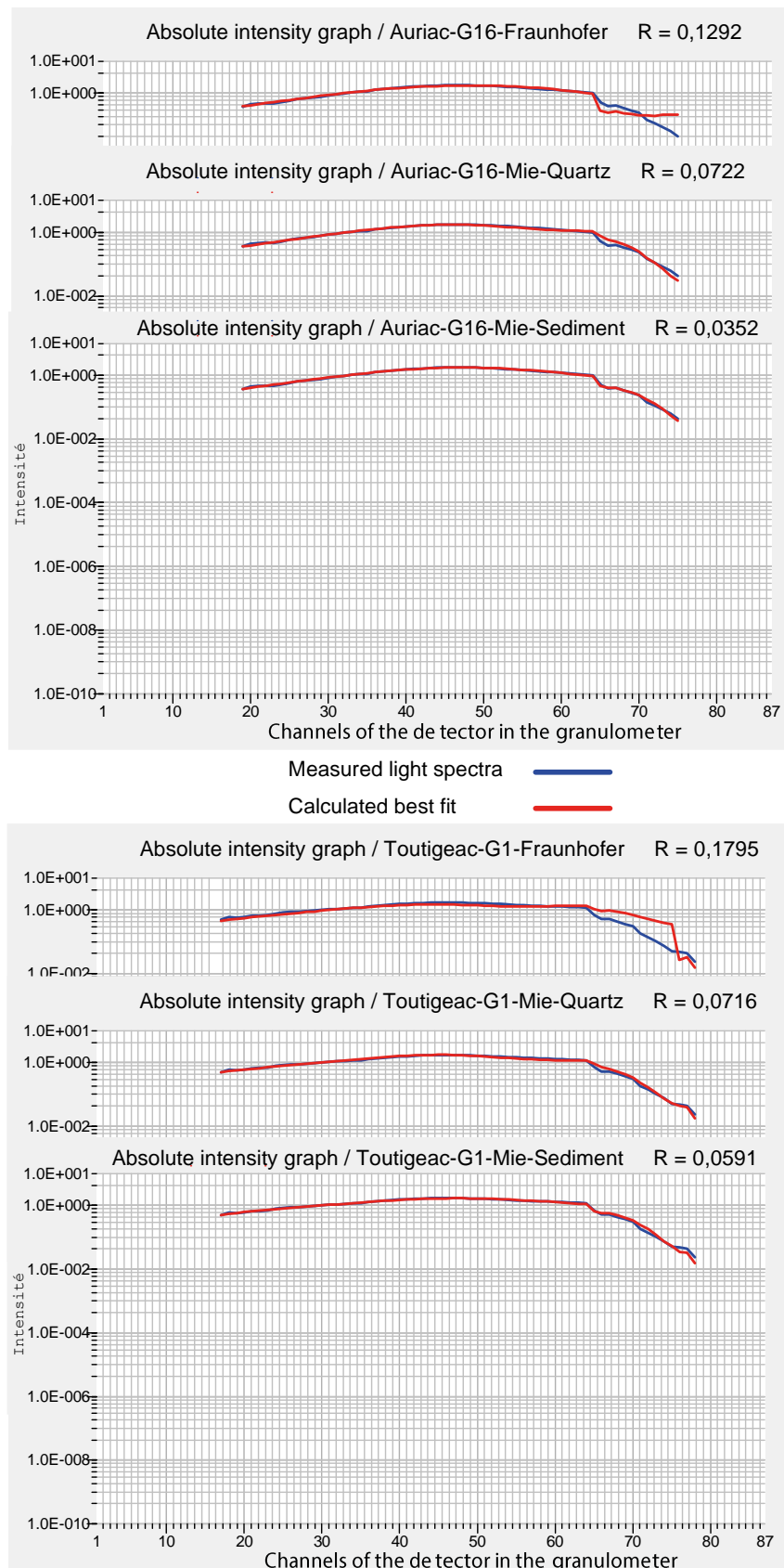


Figure SI\_2: Comparison of calculated vs. measured diagrams using different algorithms and refractive indices. The high numbered channels correspond to high angles of diffracted light mostly due to diffraction by small particles.

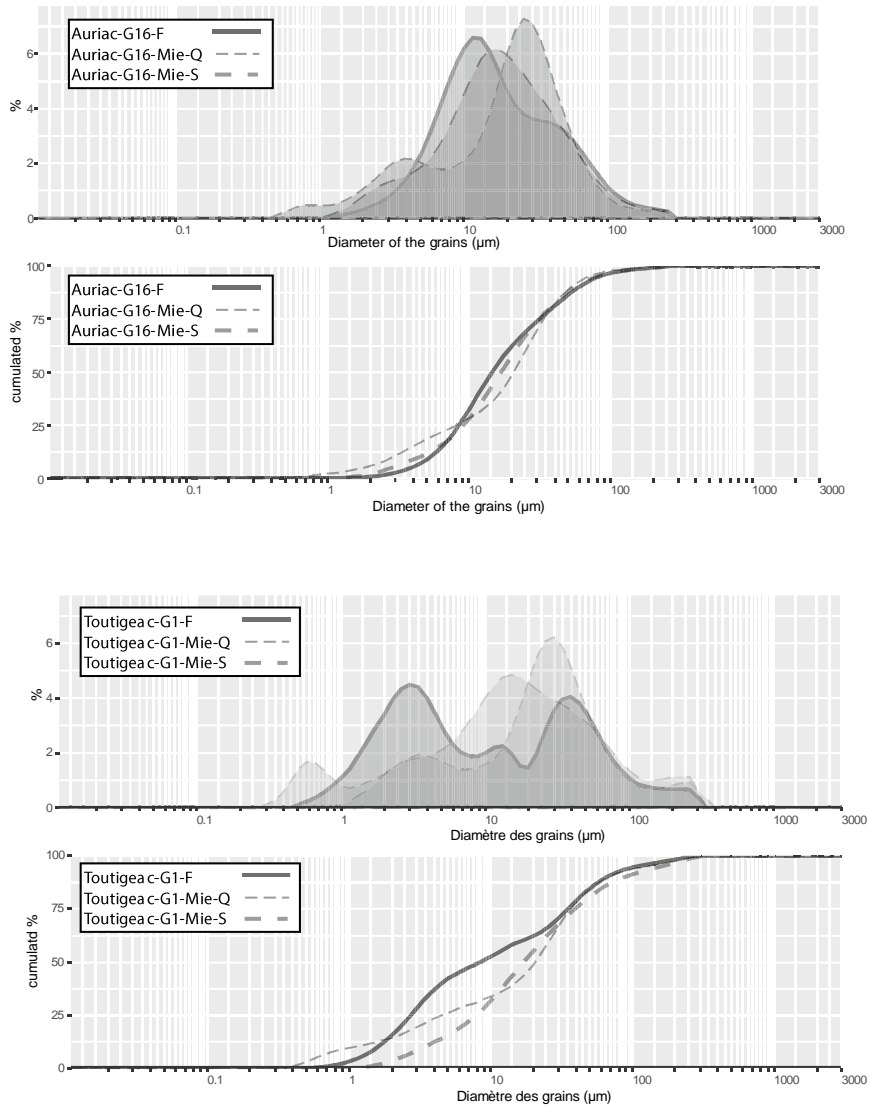


Figure SI\_3: Comparison of the particle-size distribution obtained from the calculations.